

Crucial Role of Podocyte Acid Sphingomyelinase in NLRP3 Inflammasome Activation and Glomerular Injury during Obesity

Dandan Huang

Virginia Commonwealth University

Jason M. Kidd

Virginia Commonwealth University

Yao Zou

Virginia Commonwealth University

Xiaoyuan Wu

Virginia Commonwealth University

Todd W.B. Gehr

Virginia Commonwealth University

Pin-Lan Li

Virginia Commonwealth University

Guangbi Li (✉ guangbi.li@vcuhealth.org)

Virginia Commonwealth University

Research Article

Keywords: obesity-related glomerulopathy, podocyte, NLRP3 inflammasome, exosome

Posted Date: November 28th, 2022

DOI: <https://doi.org/10.21203/rs.3.rs-2299466/v1>

License: © ⓘ This work is licensed under a Creative Commons Attribution 4.0 International License.

[Read Full License](#)

Additional Declarations: No competing interests reported.

Version of Record: A version of this preprint was published at Inflammation on July 21st, 2023. See the published version at <https://doi.org/10.1007/s10753-023-01861-y>.

Abstract

The activation of nucleotide-binding oligomerization domain-like receptor containing pyrin domain 3 (NLRP3) inflammasome has been reported to importantly contribute to glomerular inflammation and injury under different pathological conditions such as obesity. However, the mechanism mediating NLRP3 inflammasome activation in podocytes and subsequent glomerular injury remains poorly understood. Given that the ceramide signaling pathway has been reported to be implicated in obesity-related glomerulopathy (ORG), the present study was designed to test whether the ceramide producing enzyme, acid sphingomyelinase (ASM), determines NLRP3 inflammasome activation and inflammatory exosome release in podocytes leading to glomerular inflammation and injury during ORG. In *Smpd1^{trg}/Podo^{cre}* mice, podocyte-specific overexpression of *Smpd1* gene which encodes ASM significantly exaggerated high-fat diet (HFD)-induced NLRP3 inflammasome activation in podocytes and immune cell infiltration in glomeruli compared to WT/WT mice. *Smpd1* gene deletion, however, blocked these pathological changes induced by HFD in *Smpd1^{-/-}* mice. Accompanied with NLRP3 inflammasome activation and glomerular inflammation, urinary excretion of exosomes containing podocyte marker and NLRP3 inflammasome products (IL-1 β and IL-18) in *Smpd1^{trg}/Podo^{cre}* mice on the HFD was much higher than that in WT/WT mice. In contrast, *Smpd1^{-/-}* mice on the HFD had significantly lower urinary exosome excretion than WT/WT mice. Correspondingly, HFD-induced podocyte injury, glomerular sclerosis, and proteinuria were more severe in *Smpd1^{trg}/Podo^{cre}* mice, but milder in *Smpd1^{-/-}* mice compared to WT/WT mice. Using podocytes isolated from these mice, we demonstrated that visfatin, a prototype pro-inflammatory adipokine, induced NLRP3 inflammasome activation and enrichment of multivesicular bodies (MVBs) containing IL-1 β in podocytes, which was much stronger in podocytes from *Smpd1^{trg}/Podo^{cre}* mice, but weaker in those from *Smpd1^{-/-}* mice than WT/WT podocytes. By quantitative analysis of exosomes, it was found that upon visfatin stimulation podocytes from *Smpd1^{trg}/Podo^{cre}* mice released much more exosomes containing NLRP3 inflammasome products, but podocytes from *Smpd1^{-/-}* mice released much less exosomes compared to WT/WT podocytes. Super-resolution microscopy demonstrated that visfatin inhibited lysosome-MVB interaction in podocytes, indicating impaired MVB degradation by lysosome. The inhibition of lysosome-MVB interaction by visfatin was amplified by *Smpd1* gene overexpression but attenuated by *Smpd1* gene deletion. Taken together, our results suggest that ASM in podocytes is a crucial regulator of NLRP3 inflammasome activation and inflammatory exosome release that instigate glomerular inflammation and injury during obesity.

Introduction

Recent studies have shown that obesity-induced glomerular inflammation and consequent obesity-related glomerulopathy (ORG) is associated with oxidative activation of nucleotide-binding oligomerization domain-like receptor containing pyrin domain 3 (NLRP3) inflammasome, an inflammatory machinery composed of NLRP3, adaptor protein apoptosis-associated speck-like protein containing a caspase recruitment domain (ASC), and caspase-1 [1–3]. NLRP3 inflammasome activation results in proteolytical cleavage which produces active IL-1 β , IL-18, and damage-associated molecular patterns (DAMPs) [4–6].

These products of the NLRP3 inflammasome are critical to initiate local sterile inflammatory response or induce cell pyroptosis [7–10]. Previous studies have demonstrated that NLRP3 inflammasome activation in podocytes is a critical mechanism mediating glomerular inflammation and sclerosis during obesity [3, 11]. However, it remains unclear how the NLRP3 inflammasome products are secreted out of podocytes for their actions to trigger inflammatory response. Since these inflammasome products are generated in the cytoplasm but not in the endoplasmic reticulum, their release may not depend on the canonical Golgi apparatus-mediated delivery pathway as other cellular proteins or peptide factors do [12, 13]. To further understand the pathogenesis of obesity-induced glomerular inflammation, it is imperative to explore the molecular mechanisms by which NLRP3 inflammasome products are released from podocytes during obesity.

There is increasing evidence that extracellular vesicles (EVs) harbor and deliver functional molecules from secreting cells to recipient cells [14, 15]. As a subtype of EVs, exosomes are lipid bilayer-delimited small vesicles originating from the luminal membrane of multivesicular bodies (MVBs) [16]. Exosomes mediate the release of different unnecessary or harmful materials from secreting cells to maintain cellular homeostasis [17] and play an important role in cell-to-cell communication by delivery of various mRNAs, miRNAs, and proteins to recipient cells [18, 19]. It has been reported that diabetic mice had increased urinary excretion of podocyte-derived exosomes even before the development of albuminuria [20]. Also, elevation of podocyte-derived exosomes in urine has been found to be associated with albuminuria and glomerular degeneration [21–26]. Recently, we have demonstrated that increased exosome release from podocytes is associated with NLRP3 inflammasome activation in these cells during stimulation with high-level D-ribose or homocysteine [27–29]. However, it remains unknown whether obesity-induced secretion of NLRP3 inflammasome products from podocytes is mediated by exosomes.

With respect to the pathogenic mechanism of ORG, acid sphingomyelinase (ASM)-ceramide signaling pathway has been reported to contribute to NLRP3 inflammasome activation and glomerular inflammation during obesity [3]. Ceramide and its metabolites such as sphingosine-1-phosphate (S1P) have also been reported to be involved in exosome biogenesis, sorting of intraluminal vesicles (ILVs) into MVBs, and MVB fusion to plasma membrane for exosome release [30–32]. Particularly, ceramide and associated sphingolipids play a vital role in the regulation of lysosome trafficking and fusion to other intracellular vesicles in various cell types [23, 33–38]. Although several mechanisms have been reported to participate in the regulation of exosome secretion, lysosome-dependent degradation of MVBs is considered as a crucial molecular mechanism that regulates exosome release via the control of MVB fate in different cell types [39–41], including podocytes [42, 43]. The present study tested the hypothesis that NLRP3 inflammasome activation in podocytes during obesity triggers local sterile inflammation leading to ORG via an exosome secretory mechanism regulated by lysosomal ASM-ceramide signaling pathway.

Materials And Methods

Animals

Podocyte-specific Cre recombinase (Podo^{Cre}) mice were obtained from the Jackson Laboratory [Bar Harbor, ME; B6.Cg-Tg(NPHS2-Cre)295Lbh/J; stock number 008205]. Smpd1^{trg} mice are with the floxed STOP cassette inserted between the beta-actin fusion promoter and mouse cDNA, which were obtained from Dr. Erich Gulbins (University of Duisburg-Essen, Essen, Germany). Smpd1^{-/-} breeding pairs were obtained from Dr. Phillip Hylemon's laboratory at VCU [44]. The Smpd1^{trg}/Podo^{Cre} mice and their littermates were on a C57/Bl6 background. Eight-week-old male WT/WT, Smpd1^{-/-}, and Smpd1^{trg}/Podo^{Cre} mice were used in the present study. Mice were fed either low fat diet (D12450B, 10 kcal% fat, Research Diets, New Brunswick, NJ) or high fat diet (D12492, 60 kcal% fat, Research Diets, New Brunswick, NJ) for 12 weeks [11]. All protocols were approved by the Institutional Animal Care and Use Committee of the Virginia Commonwealth University.

Immunofluorescent staining

Frozen slides with mouse kidney tissue were fixed in acetone, blocked, then incubated with primary antibodies, including anti-podocin antibody (1:100; Sigma-Aldrich, St. Louis, MO), anti-desmin antibody (1:100; Invitrogen, Carlsbad, CA), anti-NLRP3 antibody (1:50; Abcam Biotechnology, Cambridge, MA), anti-ASC antibody (1:50; Santa Cruz Biotechnology, Dallas, TX), and anti-CD8 antibody (1:100; Abcam Biotechnology, Cambridge, UK), overnight at 4°C. Immunofluorescent staining was accomplished by incubating slides with Alexa-488 or Alexa-594-labeled secondary antibodies (Invitrogen, Carlsbad, CA) for 1 hour at room temperature [45]. Slides were washed, mounted, and observed by a confocal laser scanning microscope (FluoView FV1000, Olympus, Tokyo, Japan). Image Pro Plus 6.0 (Media Cybernetics, Bethesda, MD) was used to analyze colocalization which was expressed as Pearson correlation coefficient (PCC).

Immunohistochemistry

Kidneys were embedded with paraffin, 5 µm sections were cut and mounted onto microscope slides. After heat-induced antigen retrieval, washing with 3% hydrogen peroxide, and 30 min blocking with fetal bovine serum, slides were incubated with anti-IL-1β antibody (1:100; Abcam Biotechnology, Cambridge, MA), anti-IL-18 antibody (1:100; Santa Cruz Biotechnology, Dallas, TX) and anti-F4/80 antibody (1:100; Novus Biologicals, Littleton, CO), and then diluted in PBS with 4% fetal bovine serum overnight. The sections were washed with PBS and incubated with biotinylated IgG (1:200) for 1 hour at room temperature, then with streptavidin-HRP for 30 min. Each kidney section was then stained with DAB for 1 min followed by counterstaining with hematoxylin for 5 min. The slides were mounted and observed under a microscope [45].

Nanoparticle tracking analysis

Nanoparticle tracking analysis (NTA) measurements were performed with a NanoSight NTA3.2 Dev Build 3.2.16 (Malvern Instruments Ltd., UK), equipped with a sample chamber with a 638-nm laser and a Viton fluoroelastomer O-ring. The samples were injected in the sample chamber with sterile syringes (BD, New Jersey, USA) until the liquid reached the tip of the nozzle. All measurements were performed at room

temperature. The screen gain and camera level were 10 and 13, respectively. Each sample was measured at standard measurement, 30 s with manual shutter and gain adjustments. Three measurements of each sample were performed. 3D figures were exported from the software. Particles sized between 50 and 140 nm were calculated [42]. At the end of the 12-week treatment, mice were placed in metabolic cages for 24 hours to collect urine samples. After NTA, we compared urinary exosome excretion of different groups of mice in 24 hours (urinary exosome concentration/urinary creatinine concentration) vs. WT/WT-ND.

Purification and concentration of urinary exosomes

At the end of the 8-week treatment, mice were placed in metabolic cages for 24 hours to collect urine samples. Exosome purification and concentration system (ExoJuice, Columbus, OH, USA) was used to purify and concentrate urine samples for analysis. After normalization of the volume of urine samples, centrifugation at 12,000 g for 30 min was performed to remove cell debris from urine samples. The supernatant was put into an ultracentrifuge tube and 200 μ L of ExoJuice reagent was added to the bottom of the centrifuge tube. After using the centrifuge at 100,000 g for 70 min, the bottom 500 μ L of liquid was collected. When using the SW28 rotor for this step, about 230 mL of the culture supernatant was concentrated to 3 mL in one run. 3 ml of crudely extracted exosomes was mixed to 2.5 mL of sterile PBS (pH 7.2, filtered through a 0.2 μ m filter) and added to a centrifuge tube. Then, 500 μ L of ExoJuice reagent was added to the bottom of this tube. After using the centrifuge at 100,000 g for another 70 min, the centrifuge tube was taken out and 300 μ L of liquid (1) was discarded. 200 μ L of liquid (2) was collected for higher purity exosomes. Dialysis was performed to remove ExoJuice reagent from the purified exosomes with dialysis membrane with 1KD cutoff. 200 μ L of exosome extract was added to the dialysis bag against 100 mL of 1 x PBS buffer for 2 hours. Then, purified urinary exosomes were collected in the dialysis bag for analysis.

Transmission electron microscopy

For transmission electron microscopy (TEM) analysis of ultrastructural changes in podocytes, mouse kidneys were perfused with a fixative containing 3% glutaraldehyde and 4% paraformaldehyde in 0.1 mol/L phosphate buffer. After fixation and dehydration with ethanol, the samples were embedded in Durcupan resin for ultrathin sectioning by the Virginia Commonwealth University microscopy core facility [45].

Glomerular morphological examination

Fixed kidney tissues were paraffin-embedded, sectioned, and stained with periodic acid–Schiff (PAS). Fifty glomeruli per slide were counted under a light microscope and scored as 0–4 (0: no lesion, 1: sclerosis < 25%, 2: sclerosis of 25–50%, 3: sclerosis of 50–75%, 4: sclerosis > 75%) by an observer who was blind to treatment groups. Glomerular sclerosis was expressed as glomerular damage index (GDI), which was calculated by the formula $((N1 \times 1) + (N2 \times 2) + (N3 \times 3) + (N4 \times 4))/n$. N1, N2, N3, and N4 represent the numbers of glomerular damage grades 1, 2, 3, and 4, respectively, and n represents the total scored number of glomeruli [28].

Urinary protein and albumin measurements

Total urinary protein was determined spectrophotometrically by the Bradford assay (Sigma-Aldrich). Urinary albumin concentration was measured by a commercially available mouse albumin ELISA kit (Bethyl Laboratories, Montgomery, TX) [45].

Primary culture of murine podocytes

Primary culture of murine podocytes was performed as described in previous studies [46]. Briefly, we infused 20 mL of dynabeads from the abdominal aorta below the renal artery at flow rate of 7.4 mL/min/g kidney. After infusion, kidneys were removed, decapsulated, and dissected. The cortex was minced into small pieces and digested with mixture of collagenase A (1 mg/mL) and deoxyribonuclease I (0.2 mg/mL) in Hanks' balanced salt solution at 37°C for 20 min with gentle agitation. The digested tissue was placed on 100 µM strainer and gently pressed with ice-cold medium. After washing the glomeruli with ice-cold PBS 6 times, we resuspended the isolated glomeruli with beads into 5 mL medium and transferred them into the collagen I-coated culture flask. After 3 days of culture of isolated glomeruli, cellular outgrowths were detached with Trypsin-ethylenediaminetetraacetic acid solution and transferred to a glass tube. Then, the glass tube was placed onto magnetic particle concentrator for 1 min to remove the glomerular cores and dynabeads. The supernatant was passed through a 40 µm sieve to remove the remaining glomerular cores. The filtered podocytes were cultured in DMEM/F-12 (1:1) containing 10% fetal bovine serum (Cansera International, Canada) supplemented with 0.5% Insulin–Transferrin–Selenium-A liquid media supplement (Invitrogen), 100 U/ml penicillin, and 100 mg/ml streptomycin on a new collagen I-coated flask at 37°C before use in experiments. Podocytes were treated with visfatin at 2 µg/ml for 24 hours, the optimal treatment dose and time selected based on previous studies [47–50].

Structured illumination microscopy

After treatments followed by fixation, the cells were incubated with rabbit anti-Rab7a antibody (1:100; Abcam Biotechnology, Cambridge, United Kingdom) and rat anti-Lamp-1 antibody (1:100; Santa Cruz Biotechnology, Dallas, TX, USA) overnight at 4°C. After slides being washed, Alexa 488-labeled anti-rabbit secondary antibody (1:200; Life Technologies, CA, USA) and Alexa 594-labeled anti-rat secondary antibody (1:200; Life Technologies, CA, USA) were added to the cell slides and incubated for 1 hour at room temperature. Slides were then washed, stained with DAPI, and mounted. A Nikon fluorescence microscope in the structured illumination microscopy (SIM) mode was used to obtain images. Image Pro Plus 6.0 software (Media Cybernetics, Bethesda, MD, USA) was employed to analyze colocalization, expressed as the Pearson correlation coefficient [29].

Statistical analysis

SigmaPlot 14.0 was used for statistical analysis of data. All values are expressed as mean ± SEM. Significant differences among multiple groups were examined using ANOVA followed by a Student-Newman-Keuls test. $P < 0.05$ was considered statistically significant.

Results

Regulation of NLRP3 inflammasome activation in glomeruli by ASM during obesity

To test whether ASM in podocytes plays an important role in obesity-induced NLRP3 inflammasome activation in glomeruli of mice, we fed WT/WT, *Smpd1*^{-/-}, and *Smpd1*^{trg}/*Podo*^{cre} mice with normal diet (ND) or high fat diet (HFD) for 12 weeks. In *Smpd1*^{-/-} mice, *Smpd1* gene which encodes ASM was knocked out in all cells. In *Smpd1*^{trg}/*Podo*^{cre} mice, *Smpd1* gene was specifically deleted in podocytes [28]. By confocal microscopy, we observed remarkable elevation of NLRP3-ASC colocalization in glomeruli of WT/WT mice on HFD compared with ND-fed WT/WT mice, indicating the abundant formation of NLRP3 inflammasome induced by obesity. Such enhanced NLRP3 inflammasome formation in glomeruli was abolished by *Smpd1* gene knockout in *Smpd1*^{-/-} mice, but significantly amplified by podocyte-specific *Smpd1* gene overexpression in *Smpd1*^{trg}/*Podo*^{cre} mice compared to WT/WT mice (Fig. 1A). As the products of NLRP3 inflammasome, IL-1 β and IL-18 in glomeruli were measured as well. HFD treatment obviously increased IL-1 β production in glomeruli of WT/WT mice compared to ND-fed WT/WT mice (Fig. 1B). Such elevation of glomerular IL-1 β production was prevented by *Smpd1* gene deletion in *Smpd1*^{-/-} mice. On the contrary, podocyte-specific *Smpd1* gene overexpression remarkably enhanced glomerular IL-1 β production in *Smpd1*^{trg}/*Podo*^{cre} mice compared with WT/WT mice on both diets. Similar tendencies were demonstrated in glomerular IL-18 production in these mice (Fig. 1C).

Control of obesity-induced inflammatory exosome release from podocytes by ASM

To explore the mechanism by which NLRP3 inflammasome products are secreted out of podocytes to trigger glomerular inflammation during obesity, we tested whether exosomes mediate the release of NLRP3 inflammasome products from podocytes. By nanoparticle tracking analysis (NTA), we found that HFD remarkably increased urinary exosomes of WT/WT mice. Such effect of HFD on urinary exosome excretion was totally blocked by *Smpd1* gene deletion in *Smpd1*^{-/-} mice. In contrast, podocyte-specific *Smpd1* gene overexpression significantly elevated urinary exosome excretion in *Smpd1*^{trg}/*Podo*^{cre} mice on both diets (Fig. 2A and 2B). To confirm the origin of urinary exosomes detected by NTA, we measured CD63 (exosome marker) and podocin (podocyte marker) in urine samples. Mouse CD63 ELISA kit (Assay Genie, Dublin, Ireland) and mouse podocin ELISA kit (Biomatik, Cambridge, Canada) were used to detect the levels of CD63 and podocin in purified urinary exosomes. It was found that HFD-fed WT/WT mice had evidently higher levels of CD63 and podocin in their urine compared to control mice. In *Smpd1*^{-/-} mice, however, such elevations of CD63 and podocin were significantly attenuated by *Smpd1* gene knockout. On the contrary, *Smpd1* gene overexpression enhanced obesity-induced elevations of CD63 and podocin in urine of *Smpd1*^{trg}/*Podo*^{cre} mice compared with WT/WT mice (Fig. 2C and 2D). Furthermore, we confirmed whether NLRP3 inflammasome products were cargos of urinary exosomes of these mice. As

shown in Fig. 2E and 2F, HFD markedly elevated the amount of NLRP3 inflammasome products, IL-1 β and IL-18, in the urinary exosomes of WT/WT mice. Such obesity-induced elevations of IL-1 β and IL-18 in urinary exosomes were blocked by Smpd1 gene deletion in Smpd1^{-/-} mice but exaggerated by podocyte-specific Smpd1 gene overexpression in Smpd1^{trg}/Podo^{cre} mice.

Inhibition of immune cell infiltration in glomeruli by Smpd1 gene deletion during obesity

We then examined whether HFD-induced immune cell infiltration in glomeruli was determined by ASM activity in podocytes. Immunofluorescent staining of CD8, a T cell marker, revealed greater infiltration of T cells in the glomeruli of WT/WT mice on HFD compared with control mice. Such enhancement of T cell infiltration in glomeruli was prevented by Smpd1 gene deletion in Smpd1^{-/-} mice. Nevertheless, podocyte-specific Smpd1 gene overexpression significantly amplified T cell infiltration in glomeruli in Smpd1^{trg}/Podo^{cre} mice on both diets (Fig. 3A). Immunohistochemical staining of F4/80, a macrophage marker, was performed to detect macrophage infiltration in glomeruli of these mice. As shown in Fig. 3B, greater macrophage infiltration in glomeruli was detected in glomeruli of WT/WT mice on HFD compared to ND-fed WT/WT mice. Podocyte-specific Smpd1 gene overexpression significantly enhanced macrophage infiltration in glomeruli of Smpd1^{trg}/Podo^{cre} mice on both diets. On the contrary, Smpd1 gene deletion blocked obesity-induced macrophage infiltration in glomeruli of Smpd1^{-/-} mice.

Contribution of ASM activity to podocyte injury in ORG

Next, we tested whether obesity-induced podocyte injury is affected by ASM. By TEM, we observed the ultrastructure of podocytes in different groups of mice. It was found that HFD treatment induced foot process effacement in podocytes of WT/WT mice compared to control mice. Such pathological change was not observed in Smpd1^{-/-} mice on HFD. Podocyte-specific Smpd1 gene overexpression, however, worsened obesity-induced foot process effacement in podocytes of Smpd1^{trg}/Podo^{cre} mice (Fig. 4A). Also, we found that HFD-fed WT/WT mice had much less expression of podocin (a protein component of the filtration slits of podocytes) in glomeruli compared with ND-fed WT/WT mice. On the contrary, glomerular expression of desmin, a marker of podocyte injury, was obviously increased by HFD treatment in WT/WT mice. Such pathological changes in podocin and desmin were totally blocked by Smpd1 gene knockout, but significantly amplified by podocyte-specific Smpd1 gene overexpression (Fig. 4B and 4C).

Glomerular damage and proteinuria prevented by Smpd1 gene deletion

Moreover, morphological and functional changes of glomeruli were assessed in different groups of mice. By PAS staining, morphological examinations showed sclerotic changes in glomeruli of WT/WT mice on

HFD. HFD treatment significantly increased the glomerular damage index in WT/WT mice. *Smpd1* gene knockout blocked the glomerular damage induced by obesity. Podocyte-specific *Smpd1* gene overexpression, however, enhanced glomerular damage in *Smpd1^{trg}/Podo^{cre}* mice on both diets (Fig. 5A). Meanwhile, HFD-fed WT/WT mice on HFD exhibited proteinuria and albuminuria compared to ND-fed WT/WT mice. Proteinuria and albuminuria due to obesity were prevented by *Smpd1* gene deletion in *Smpd1^{-/-}* mice. On the contrary, podocyte-specific *Smpd1* gene overexpression significantly aggravated obesity-induced proteinuria and albuminuria in *Smpd1^{trg}/Podo^{cre}* mice.

Visfatin-induced NLRP3 inflammasome activation in podocytes determined by ASM

As a pro-inflammatory adipokine, visfatin has been reported to play an important role in obesity-induced chronic inflammation [51]. Therefore, we tested whether visfatin is involved in NLRP3 inflammasome activation and associated inflammatory exosome release in podocytes. By confocal microscopy, we demonstrated that visfatin induced formation of NLRP3 inflammasomes as indicated by increased colocalization of NLRP3 (green fluorescence) and ASC (red fluorescence) in WT/WT podocytes compared to control cells. In podocytes isolated from *Smpd1^{-/-}* mice, visfatin-induced NLRP3 inflammasome activation was blocked by *Smpd1* gene deletion. In contrast, *Smpd1* gene overexpression enhanced visfatin-induced NLRP3 inflammasome activation in podocytes of *Smpd1^{trg}/Podo^{cre}* mice (Fig. 6).

Elevation of inflammatory exosome release from podocytes by visfatin

To test whether visfatin can induce inflammatory exosome release from podocytes, we observed Rab7a, an MVB marker, and IL-1 β , a NLRP3 inflammasome product, in podocytes by confocal microscopy. As shown in Fig. 7A and 7B, there was much more colocalization of Rab7a (green fluorescence) and IL-1 β (red fluorescence) in WT/WT podocytes treated with visfatin compared to control cells, indicating formation of MVBs containing IL-1 β . Such increase in colocalization of Rab7a and IL-1 β was prevented by *Smpd1* gene knockout in podocytes of *Smpd1^{-/-}* mice. However, *Smpd1* gene overexpression amplified such change in podocytes of *Smpd1^{trg}/Podo^{cre}* mice. By NTA, we also measured exosome release from different podocytes. It was found that visfatin evidently increased exosome secretion from WT/WT podocytes. Such elevation of exosome release was blocked by *Smpd1* gene deletion but aggravated by *Smpd1* gene overexpression (Fig. 7C and 7D). Moreover, mouse CD63 ELISA kit (Assay Genie, Dublin, Ireland), mouse IL-1 β ELISA kit (Assay Genie, Dublin, Ireland), and mouse IL-18 ELISA kit (Assay Genie, Dublin, Ireland) were used to detect the levels of CD63, IL-1 β , and IL-18 in purified exosomes. As shown in Fig. 7E-G, CD63, IL-1 β , and IL-18 were elevated by visfatin in purified exosomes. Such changes were significantly attenuated by *Smpd1* gene deletion in podocytes of *Smpd1^{-/-}* mice. On

the contrary, Smpd1 gene overexpression in podocytes enhanced visfatin-induced elevations of CD63, IL-1 β , and IL-18 in purified exosomes.

Inhibition of lysosome-MVB interaction in podocytes by visfatin

To explore the molecular mechanism by which visfatin affects exosome release from podocytes, we observed Rab7a, an MVB marker, and Lamp-1, a lysosome marker, in podocytes by super-resolution microscopy. As shown in Fig. 8, there was considerable amount of colocalization of Rab7a (green fluorescence) and Lamp-1 (red fluorescence) in WT/WT podocytes under control condition, indicating normal lysosome-MVB interaction. Visfatin obviously decreased the colocalization of Rab7a and Lamp-1 in WT/WT podocytes, suggesting reduction of lysosome-MVB interaction. Such change of lysosome-MVB interaction was prevented by Smpd1 gene deletion in podocytes of Smpd1^{-/-} mice. However, Smpd1 gene overexpression amplified visfatin-induced reduction of lysosome-MVB interaction in podocytes of Smpd1^{trg}/Podo^{cre} mice.

Discussion

The major goal of the present study was to determine whether the ceramide producing enzyme, ASM, determines NLRP3 inflammasome activation and inflammatory exosome release in podocytes leading to glomerular inflammation and injury during ORG. It was found that HFD treatment concurrently induced NLRP3 inflammasome activation and abundant urinary exosome excretion. The large amounts of podocyte marker and NLRP3 inflammasome product were detected in these exosomes, suggesting that the release of NLRP3 inflammasome products from podocytes was mediated by exosomes. These pathological changes were associated with glomerular inflammation, podocyte injury, and proteinuria in HFD-fed mice. In vitro, visfatin as a pro-inflammatory adipokine activated NLRP3 inflammasome and enhanced exosome release in podocytes simultaneously. Moreover, lysosome-MVB interaction in podocytes was inhibited by visfatin, indicating the slowdown of lysosome-dependent degradation of MVBs in these cells. Results collected from WT/WT, Smpd1^{-/-}, and Smpd1^{trg}/Podo^{cre} mice and podocytes of these mice revealed that ASM-ceramide signaling pathway was importantly involved in the regulation of NLRP3 inflammasome activation and inflammatory exosome release in podocytes during obesity and thereby determined the development of glomerular inflammation and ORG.

ORG is an increasing cause of renal failure [52]. Although, the pathogenic mechanisms of ORG remain incompletely understood. Potential mechanisms by which obesity induces renal injury include insulin resistance, hyperlipidemia, altered renal hemodynamics, activation of renin-angiotensin-aldosterone system, oxidative stress, and inflammation [52]. It has been reported that glomerular inflammation and oxidative stress can cause glomerular dysfunction and albuminuria in obese rats even in the early stage of obesity [53]. Recently, NLRP3 inflammasome, an intracellular inflammatory machinery, in podocytes has been demonstrated to be essential for the initiation of chronic sterile inflammation in the glomeruli of

obese mice [11]. Gene knockout of ASC, a NLRP3 inflammasome component, can remarkably attenuate obesity-induced glomerular inflammation, podocyte injury, and proteinuria in mice [11]. However, the molecular mechanism by which NLRP3 inflammasome products in podocytes are released during obesity remains unclear. In the present study, we demonstrated that NLRP3 inflammasome activation was associated with abundant exosome secretion in the podocytes of obese mice. Moreover, these podocyte-derived exosomes contained large amount of inflammatory cytokines. To our knowledge, these results represent the first experimental evidence that obesity-induced NLRP3 inflammasome product release from podocytes may be attributed to the exosome secretory mechanism. In previous studies, some signaling pathways have been proposed to regulate NLRP3 inflammasome activation in podocytes during obesity, such as P2X7 receptor, reactive oxygen species (ROS), and NF- κ B [54, 55]. Although, little is known so far how NLRP3 inflammasome activation in podocytes leads to chronic sterile inflammation in glomeruli during obesity. Our findings suggest that podocyte-derived exosomes containing NLRP3 inflammasome may trigger glomerular inflammation during obesity and thereby initiate the development of ORG.

We also examined whether ASM-ceramide signaling pathway is involved in the regulation of NLRP3 inflammasome activation and inflammatory exosome release in podocytes during obesity. It was demonstrated that *Smpd1* gene deletion blocked obesity-induced activation of NLRP3 inflammasome and elevation of exosome secretion from podocytes, which was associated with attenuated glomerular inflammation, podocyte injury, and proteinuria. On the contrary, podocyte-specific *Smpd1* gene overexpression aggravated obesity-induced pathological changes in the NLRP3 inflammasome and exosome release, which was accompanied by amplified glomerular inflammatory response, podocyte damage, and glomerular injury. These results suggest that the pathological role of ASM-ceramide signaling pathway in obesity-induced glomerular inflammation and injury is attributed to NLRP3 inflammasome activation and increased exosome release in podocytes. To our knowledge, these results provide the first evidence that exosome secretion from podocytes may serve as a critical mechanism activating or enhancing glomerular inflammation and injury during obesity. In previous studies, ceramide production by ASM was shown to be critical for obesity-induced superoxide production and NLRP3 inflammasome activation in glomeruli, leading to glomerular inflammation and injury in HFD-fed mice [3, 56]. In addition, activation of NLRP3 inflammasome and elevation of exosome secretion have been found in podocytes stimulated with high levels of D-ribose and homocysteine [27, 29, 57], suggesting that exosome secretory mechanism may mediate the release of NLRP3 inflammasome products from podocytes during different metabolic syndromes. More recently, gasdermin D (GSDMD) pore formation has been reported to contribute to the release of inflammasome products [58, 59]. The enhancement of GSDMD pore formation may lead to cell pyroptosis [60–62]. It has been reported that GSDMD pore contributes to the development of obesity-associated hepatocellular carcinoma [63] and non-alcoholic fatty liver disease [64, 65]. However, it remains unknown whether obesity induces GSDMD pore formation on the plasma membrane of podocytes. In our future study, it would be interesting to test whether ASM-ceramide signaling pathway regulates GSDMD pore formation to determine NLRP3 inflammasome product release and pyroptosis in podocytes during obesity.

After confirmation of increased exosome release from podocytes during obesity, we went on to address how inflammatory exosome secretion from podocytes was regulated in ORG. The lysosome in podocytes and other cells has been demonstrated to actively respond to extracellular or intracellular stress such as increased MVBs, autophagosomes, or pathological stimuli [16, 66]. Although several mechanisms have been reported to participate in the regulation of exosome release, lysosome-dependent degradation of MVBs is considered a crucial molecular mechanism to regulate exosome secretion via the control of MVB fate [39–41]. Recently, we have demonstrated that secretion of inflammatory exosomes from podocytes is determined by lysosome function during stimulation with high-level D-ribose or homocysteine [27–29]. In the present study, we found that visfatin, a pro-inflammatory adipokine, activated the NLRP3 inflammasome and enhanced exosome release in podocytes simultaneously. Moreover, lysosome-MVB interaction in podocytes was inhibited by visfatin, indicating the slowdown of lysosome-dependent degradation of MVBs in these cells. The inhibition of lysosome-MVB interaction in podocytes was prevented by *Smpd1* gene deletion but aggravated by *Smpd1* gene overexpression. In studies using coronary endothelial cells, visfatin has been demonstrated to enhance the fusion of lysosomes to plasma membrane, leading to ASM translocation, ceramide accumulation, membrane raft clustering, and NADPH oxidase activation [49]. Also, it has been reported that the formation and activation of NLRP3 inflammasomes by visfatin may be an important initiating mechanism of the endothelial inflammatory response leading to arterial inflammation and endothelial dysfunction in mice during early-stage obesity [67]. More recently, visfatin has been shown to induce NLRP3 inflammasome activation in podocytes [47]. Our findings together with these previous results provide strong evidence that inhibition of lysosome function may lead to the slowdown of lysosome-dependent MVB degradation and thereby enhances exosome secretion in podocytes, leading to the acceleration of exosome-mediated NLRP3 inflammasome product release. Moreover, our findings suggest that ASM exerts an important regulatory role on lysosome function and that enhancement of ASM activity may result in inhibition of lysosome function, reduction of lysosome-MVB interaction, and elevation of exosome release in podocytes. To our knowledge, there have been no reports on the role of ASM-ceramide signaling pathway in the regulation of lysosome function in podocytes during obesity. Our results provide direct evidence that ASM critically contributes to visfatin-induced elevation of exosome release through the inhibition of lysosome function in podocytes. Recently, we have demonstrated that endogenously produced ROS importantly contributes to reduction of lysosome-MVB interaction and elevation of exosome secretion from podocytes through inhibition of TRPML1 channel activity [29]. Given the implication of visfatin and ASM in NADPH oxidase activation [49], it is possible that ASM may determine visfatin-induced inflammatory exosome release via regulation of superoxide production by NADPH oxidase in podocytes.

In summary, the present study revealed a new triggering mechanism of glomerular inflammation during obesity, which is characterized by NLRP3 inflammasome activation, reduced lysosome-MVB interaction, and increased exosome secretion in podocytes. The release of exosomes containing NLRP3 inflammasome products from podocytes may represent a novel early event leading to immune cell infiltration, initiating glomerular inflammation and injury, ultimately resulting in ORG and renal failure.

These results may direct toward the development of new therapeutic strategies targeting exosome release from podocytes for prevention or treatment of glomerular inflammation and injury during obesity.

Declarations

Competing Interests

The authors declare no competing interests.

Contributions

Conceptualization: Pin-Lan Li and Guangbi Li. Methodology: Dandan Huang, Yao Zou, Xiaoyuan Wu, and Guangbi Li. Formal analysis and investigation: Dandan Huang and Guangbi Li. Writing - original draft preparation: Dandan Huang and Guangbi Li. Writing - review and editing: Jason M. Kidd, Todd W.B. Gehr, and Pin-Lan Li. All authors read and approved the final manuscript.

Funding

This study was supported by NIH grants DK054927 and DK120491.

Availability of Data and Materials

The data used to support the findings of this study are available from the corresponding author upon request.

References

1. Martinon F, Mayor A, Tschopp J. The inflammasomes: guardians of the body. *Annu Rev Immunol* 2009, 27:229-65.
2. Abais JM, Zhang C, Xia M, Liu Q, Gehr TW, Boini KM, et al. NADPH oxidase-mediated triggering of inflammasome activation in mouse podocytes and glomeruli during hyperhomocysteinemia. *Antioxidants & redox signaling* 2013, 18:1537-48.
3. Boini KM, Xia M, Koka S, Gehr TW, Li PL. Instigation of NLRP3 inflammasome activation and glomerular injury in mice on the high fat diet: role of acid sphingomyelinase gene. *Oncotarget* 2016, 7:19031-44.
4. Cruz CM, Rinna A, Forman HJ, Ventura AL, Persechini PM, Ojcius DM. ATP activates a reactive oxygen species-dependent oxidative stress response and secretion of proinflammatory cytokines in macrophages. *J Biol Chem* 2007, 282:2871-9.
5. Halle A, Hornung V, Petzold GC, Stewart CR, Monks BG, Reinheckel T, et al. The NALP3 inflammasome is involved in the innate immune response to amyloid-beta. *Nat Immunol* 2008, 9:857-65.

6. Nour AM, Yeung YG, Santambrogio L, Boyden ED, Stanley ER, Brojatsch J. Anthrax lethal toxin triggers the formation of a membrane-associated inflammasome complex in murine macrophages. *Infect Immun* 2009, 77:1262-71.
7. Chen GY, Nunez G. Sterile inflammation: sensing and reacting to damage. *Nat Rev Immunol* 2010, 10:826-37.
8. Lamkanfi M. Emerging inflammasome effector mechanisms. *Nat Rev Immunol* 2011, 11:213-20.
9. Martinon F, Burns K, Tschopp J. The inflammasome: a molecular platform triggering activation of inflammatory caspases and processing of proIL-beta. *Mol Cell* 2002, 10:417-26.
10. Srinivasula SM, Poyet JL, Razmara M, Datta P, Zhang Z, Alnemri ES. The PYRIN-CARD protein ASC is an activating adaptor for caspase-1. *J Biol Chem* 2002, 277:21119-22.
11. Boini KM, Xia M, Abais JM, Li G, Pitzer AL, Gehr TW, et al. Activation of inflammasomes in podocyte injury of mice on the high fat diet: Effects of ASC gene deletion and silencing. *Biochim Biophys Acta* 2014, 1843:836-45.
12. Griffiths G, Simons K. The trans Golgi network: sorting at the exit site of the Golgi complex. *Science* 1986, 234:438-43.
13. Gu F, Crump CM, Thomas G. Trans-Golgi network sorting. *Cellular and molecular life sciences : CMLS* 2001, 58:1067-84.
14. Colombo M, Raposo G, Thery C. Biogenesis, secretion, and intercellular interactions of exosomes and other extracellular vesicles. *Annu Rev Cell Dev Biol* 2014, 30:255-89.
15. Schorey JS, Harding CV. Extracellular vesicles and infectious diseases: new complexity to an old story. *J Clin Invest* 2016, 126:1181-9.
16. Li G, Kidd J, Li PL. Podocyte Lysosome Dysfunction in Chronic Glomerular Diseases. *International journal of molecular sciences* 2020, 21.
17. Takahashi A, Okada R, Nagao K, Kawamata Y, Hanyu A, Yoshimoto S, et al. Exosomes maintain cellular homeostasis by excreting harmful DNA from cells. *Nat Commun* 2017, 8:15287.
18. Eitan E, Suire C, Zhang S, Mattson MP. Impact of lysosome status on extracellular vesicle content and release. *Ageing research reviews* 2016, 32:65-74.
19. van Balkom BW, Pisitkun T, Verhaar MC, Knepper MA. Exosomes and the kidney: prospects for diagnosis and therapy of renal diseases. *Kidney Int* 2011, 80:1138-45.
20. Zhou H, Kajiyama H, Tsuji T, Hu X, Leelahavanichkul A, Vento S, et al. Urinary exosomal Wilms' tumor-1 as a potential biomarker for podocyte injury. *Am J Physiol Renal Physiol* 2013, 305:F553-9.
21. Erdbrugger U, Le TH. Extracellular Vesicles in Renal Diseases: More than Novel Biomarkers? *J Am Soc Nephrol* 2016, 27:12-26.
22. Hara M, Yanagihara T, Kihara I, Higashi K, Fujimoto K, Kajita T. Apical cell membranes are shed into urine from injured podocytes: a novel phenomenon of podocyte injury. *Journal of the American Society of Nephrology : JASN* 2005, 16:408-16.

23. Lee H, Han KH, Lee SE, Kim SH, Kang HG, Cheong HI. Urinary exosomal WT1 in childhood nephrotic syndrome. *Pediatr Nephrol* 2012, 27:317-20.
24. Lytvyn Y, Xiao F, Kennedy CR, Perkins BA, Reich HN, Scholey JW, et al. Assessment of urinary microparticles in normotensive patients with type 1 diabetes. *Diabetologia* 2017, 60:581-584.
25. Stahl AL, Johansson K, Mossberg M, Kahn R, Karpman D. Exosomes and microvesicles in normal physiology, pathophysiology, and renal diseases. *Pediatric nephrology* 2019, 34:11-30.
26. Tkaczyk M, Baj Z. Surface markers of platelet function in idiopathic nephrotic syndrome in children. *Pediatric nephrology* 2002, 17:673-7.
27. Hong J, Bhat OM, Li G, Dempsey SK, Zhang Q, Ritter JK, et al. Lysosomal regulation of extracellular vesicle excretion during d-ribose-induced NLRP3 inflammasome activation in podocytes. *Biochim Biophys Acta Mol Cell Res* 2019, 1866:849-860.
28. Huang D, Li G, Zhang Q, Bhat OM, Zou Y, Ritter JK, et al. Contribution of podocyte inflammatory exosome release to glomerular inflammation and sclerosis during hyperhomocysteinemia. *Biochimica et biophysica acta Molecular basis of disease* 2021, 1867:166146.
29. Li G, Huang D, Li N, Ritter JK, Li PL. Regulation of TRPML1 channel activity and inflammatory exosome release by endogenously produced reactive oxygen species in mouse podocytes. *Redox Biol* 2021, 43:102013.
30. Kajimoto T, Okada T, Miya S, Zhang L, Nakamura S. Ongoing activation of sphingosine 1-phosphate receptors mediates maturation of exosomal multivesicular endosomes. *Nature communications* 2013, 4:2712.
31. Trajkovic K, Hsu C, Chiantia S, Rajendran L, Wenzel D, Wieland F, et al. Ceramide triggers budding of exosome vesicles into multivesicular endosomes. *Science* 2008, 319:1244-7.
32. Yuyama K, Sun H, Mitsutake S, Igarashi Y. Sphingolipid-modulated exosome secretion promotes clearance of amyloid-beta by microglia. *The Journal of biological chemistry* 2012, 287:10977-89.
33. Alvarez-Erviti L, Seow Y, Schapira AH, Gardiner C, Sargent IL, Wood MJ, et al. Lysosomal dysfunction increases exosome-mediated alpha-synuclein release and transmission. *Neurobiol Dis* 2011, 42:360-7.
34. Cui Y, Luan J, Li H, Zhou X, Han J. Exosomes derived from mineralizing osteoblasts promote ST2 cell osteogenic differentiation by alteration of microRNA expression. *FEBS Lett* 2016, 590:185-92.
35. Lee MJ, Van Brocklyn JR, Thangada S, Liu CH, Hand AR, Menzeleev R, et al. Sphingosine-1-phosphate as a ligand for the G protein-coupled receptor EDG-1. *Science* 1998, 279:1552-5.
36. Li PL, Zhang Y, Abais JM, Ritter JK, Zhang F. Cyclic ADP-Ribose and NAADP in Vascular Regulation and Diseases. *Messenger* 2013, 2:63-85.
37. Liebau MC, Braun F, Hopker K, Weitbrecht C, Bartels V, Muller RU, et al. Dysregulated autophagy contributes to podocyte damage in Fabry's disease. *PLoS One* 2013, 8:e63506.
38. Lorber D. Importance of cardiovascular disease risk management in patients with type 2 diabetes mellitus. *Diabetes Metab Syndr Obes* 2014, 7:169-83.

39. Boulanger CM, Loyer X, Rautou PE, Amabile N. Extracellular vesicles in coronary artery disease. *Nat Rev Cardiol* 2017, 14:259-272.
40. Chistiakov DA, Orekhov AN, Bobryshev YV. Extracellular vesicles and atherosclerotic disease. *Cellular and molecular life sciences : CMLS* 2015, 72:2697-708.
41. Hessvik NP, Llorente A. Current knowledge on exosome biogenesis and release. *Cell Mol Life Sci* 2018, 75:193-208.
42. Li G, Huang D, Hong J, Bhat OM, Yuan X, Li PL. Control of lysosomal TRPML1 channel activity and exosome release by acid ceramidase in mouse podocytes. *American journal of physiology Cell physiology* 2019, 317:C481-C491.
43. Li G, Huang D, Bhat OM, Poklis JL, Zhang A, Zou Y, et al. Abnormal podocyte TRPML1 channel activity and exosome release in mice with podocyte-specific *Asah1* gene deletion. *Biochimica et biophysica acta Molecular and cell biology of lipids* 2020, 1866:158856.
44. Gupta S, Natarajan R, Payne SG, Studer EJ, Spiegel S, Dent P, et al. Deoxycholic acid activates the c-Jun N-terminal kinase pathway via FAS receptor activation in primary hepatocytes. Role of acidic sphingomyelinase-mediated ceramide generation in FAS receptor activation. *The Journal of biological chemistry* 2004, 279:5821-8.
45. Li G, Kidd J, Kaspar C, Dempsey S, Bhat OM, Camus S, et al. Podocytopathy and Nephrotic Syndrome in Mice with Podocyte-Specific Deletion of the *Asah1* Gene: Role of Ceramide Accumulation in Glomeruli. *The American journal of pathology* 2020, 190:1211-1223.
46. Li G, Huang D, Bhat OM, Poklis JL, Zhang A, Zou Y, et al. Abnormal podocyte TRPML1 channel activity and exosome release in mice with podocyte-specific *Asah1* gene deletion. *Biochimica et biophysica acta Molecular and cell biology of lipids* 2021, 1866:158856.
47. Koka S, Xia M, Zhang C, Zhang Y, Li PL, Boini KM. Podocyte NLRP3 Inflammasome Activation and Formation by Adipokine Visfatin. *Cellular physiology and biochemistry : international journal of experimental cellular physiology, biochemistry, and pharmacology* 2019, 53:355-365.
48. Chen Y, Pitzer AL, Li X, Li PL, Wang L, Zhang Y. Instigation of endothelial *Nlrp3* inflammasome by adipokine visfatin promotes inter-endothelial junction disruption: role of HMGB1. *Journal of cellular and molecular medicine* 2015, 19:2715-27.
49. Xia M, Zhang C, Boini KM, Thacker AM, Li PL. Membrane raft-lysosome redox signalling platforms in coronary endothelial dysfunction induced by adipokine visfatin. *Cardiovascular research* 2011, 89:401-9.
50. Boini KM, Zhang C, Xia M, Han WQ, Brimson C, Poklis JL, et al. Visfatin-induced lipid raft redox signaling platforms and dysfunction in glomerular endothelial cells. *Biochimica et biophysica acta* 2010, 1801:1294-304.
51. Tilg H, Moschen AR. Role of adiponectin and PBEF/visfatin as regulators of inflammation: involvement in obesity-associated diseases. *Clinical science* 2008, 114:275-88.
52. Tang J, Yan H, Zhuang S. Inflammation and oxidative stress in obesity-related glomerulopathy. *International journal of nephrology* 2012, 2012:608397.

53. Mima A, Yasuzawa T, King GL, Ueshima S. Obesity-associated glomerular inflammation increases albuminuria without renal histological changes. *FEBS open bio* 2018, 8:664-670.
54. Hou XX, Dong HR, Sun LJ, Yang M, Cheng H, Chen YP. Purinergic 2X7 Receptor is Involved in the Podocyte Damage of Obesity-Related Glomerulopathy via Activating Nucleotide-Binding and Oligomerization Domain-Like Receptor Protein 3 Inflammasome. *Chinese medical journal* 2018, 131:2713-2725.
55. Xu X, Huang X, Zhang L, Huang X, Qin Z, Hua F. Adiponectin protects obesity-related glomerulopathy by inhibiting ROS/NF-kappaB/NLRP3 inflammation pathway. *BMC nephrology* 2021, 22:218.
56. Boini KM, Zhang C, Xia M, Poklis JL, Li PL. Role of sphingolipid mediator ceramide in obesity and renal injury in mice fed a high-fat diet. *The Journal of pharmacology and experimental therapeutics* 2010, 334:839-46.
57. Huang D, Li G, Bhat OM, Zou Y, Li N, Ritter JK, et al. Exosome Biogenesis and Lysosome Function Determine Podocyte Exosome Release and Glomerular Inflammatory Response during Hyperhomocysteinemia. *The American journal of pathology* 2022, 192:43-55.
58. Evavold CL, Ruan J, Tan Y, Xia S, Wu H, Kagan JC. The Pore-Forming Protein Gasdermin D Regulates Interleukin-1 Secretion from Living Macrophages. *Immunity* 2018, 48:35-44 e6.
59. He WT, Wan H, Hu L, Chen P, Wang X, Huang Z, et al. Gasdermin D is an executor of pyroptosis and required for interleukin-1beta secretion. *Cell research* 2015, 25:1285-98.
60. Carta S, Tassi S, Pettinati I, Delfino L, Dinarello CA, Rubartelli A. The rate of interleukin-1beta secretion in different myeloid cells varies with the extent of redox response to Toll-like receptor triggering. *J Biol Chem* 2011, 286:27069-80.
61. Carta S, Penco F, Lavieri R, Martini A, Dinarello CA, Gattorno M, et al. Cell stress increases ATP release in NLRP3 inflammasome-mediated autoinflammatory diseases, resulting in cytokine imbalance. *Proc Natl Acad Sci U S A* 2015, 112:2835-40.
62. Liston A, Masters SL. Homeostasis-altering molecular processes as mechanisms of inflammasome activation. *Nat Rev Immunol* 2017, 17:208-214.
63. Yamagishi R, Kamachi F, Nakamura M, Yamazaki S, Kamiya T, Takasugi M, et al. Gasdermin D-mediated release of IL-33 from senescent hepatic stellate cells promotes obesity-associated hepatocellular carcinoma. *Science immunology* 2022, 7:eabl7209.
64. Rodriguez-Antonio I, Lopez-Sanchez GN, Uribe M, Chavez-Tapia NC, Nuno-Lambarri N. Role of the inflammasome, gasdermin D, and pyroptosis in non-alcoholic fatty liver disease. *Journal of gastroenterology and hepatology* 2021, 36:2720-2727.
65. Xu B, Jiang M, Chu Y, Wang W, Chen D, Li X, et al. Gasdermin D plays a key role as a pyroptosis executor of non-alcoholic steatohepatitis in humans and mice. *Journal of hepatology* 2018, 68:773-782.
66. Settembre C, Ballabio A. Lysosomal adaptation: how the lysosome responds to external cues. *Cold Spring Harbor perspectives in biology* 2014, 6.

67. Xia M, Boini KM, Abais JM, Xu M, Zhang Y, Li PL. Endothelial NLRP3 inflammasome activation and enhanced neointima formation in mice by adipokine visfatin. *The American journal of pathology* 2014, 184:1617-28.

Figures

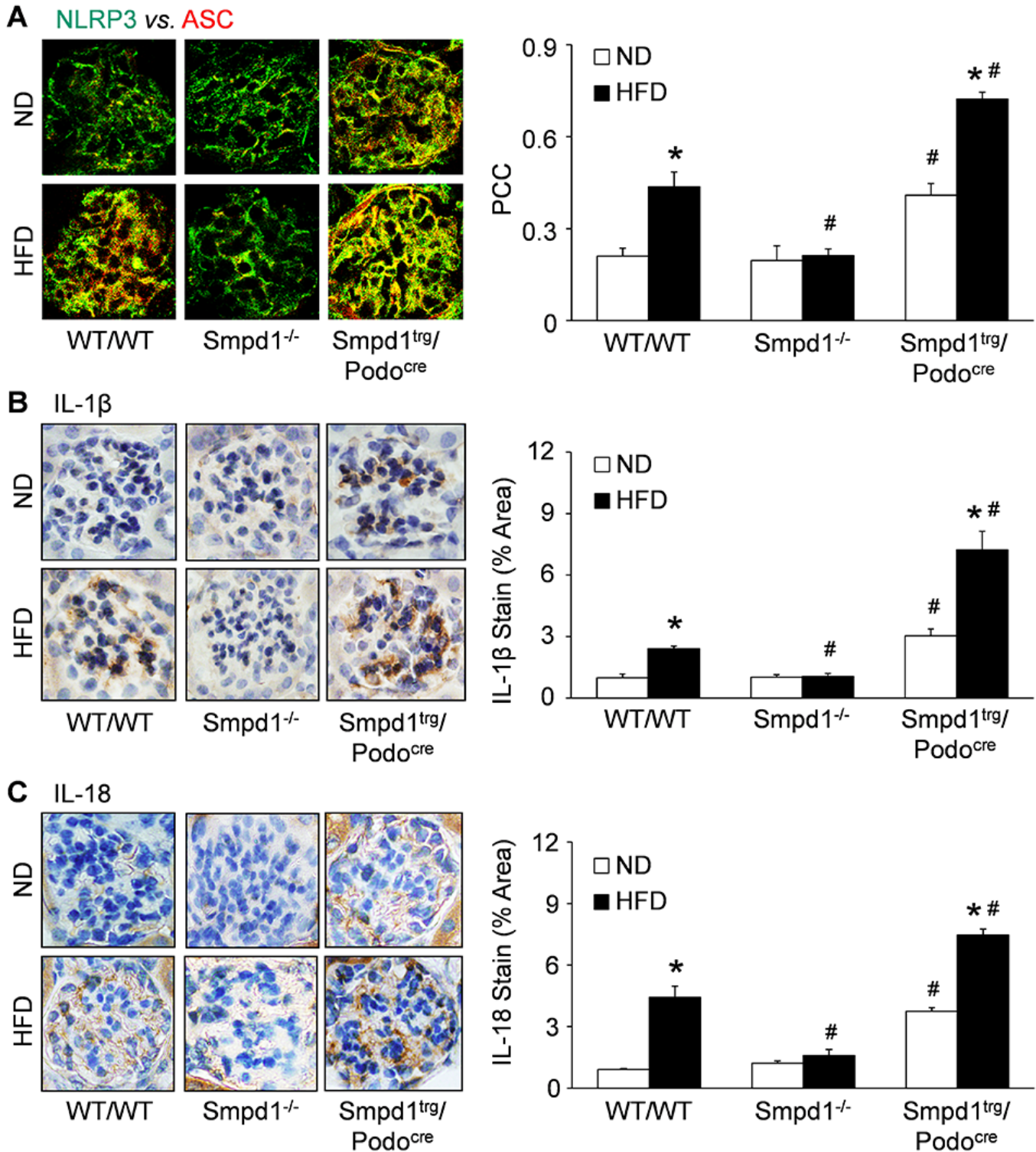


Figure 1

HFD-induced NLRP3 inflammasome activation in glomeruli abolished by *Smpd1* gene deletion. A. Representative images and summarized data showing the colocalization of NLRP3 and ASC in glomeruli of different groups of mice (n=3-5). B. Representative images and summarized data showing the immunohistochemical staining of IL-1 β in glomeruli of different groups of mice (n=4). C. Representative images and summarized data showing the immunohistochemical staining of IL-18 in glomeruli of different groups of mice (n=6). * P<0.05 vs. ND group. # P<0.05 vs. WT/WT group.

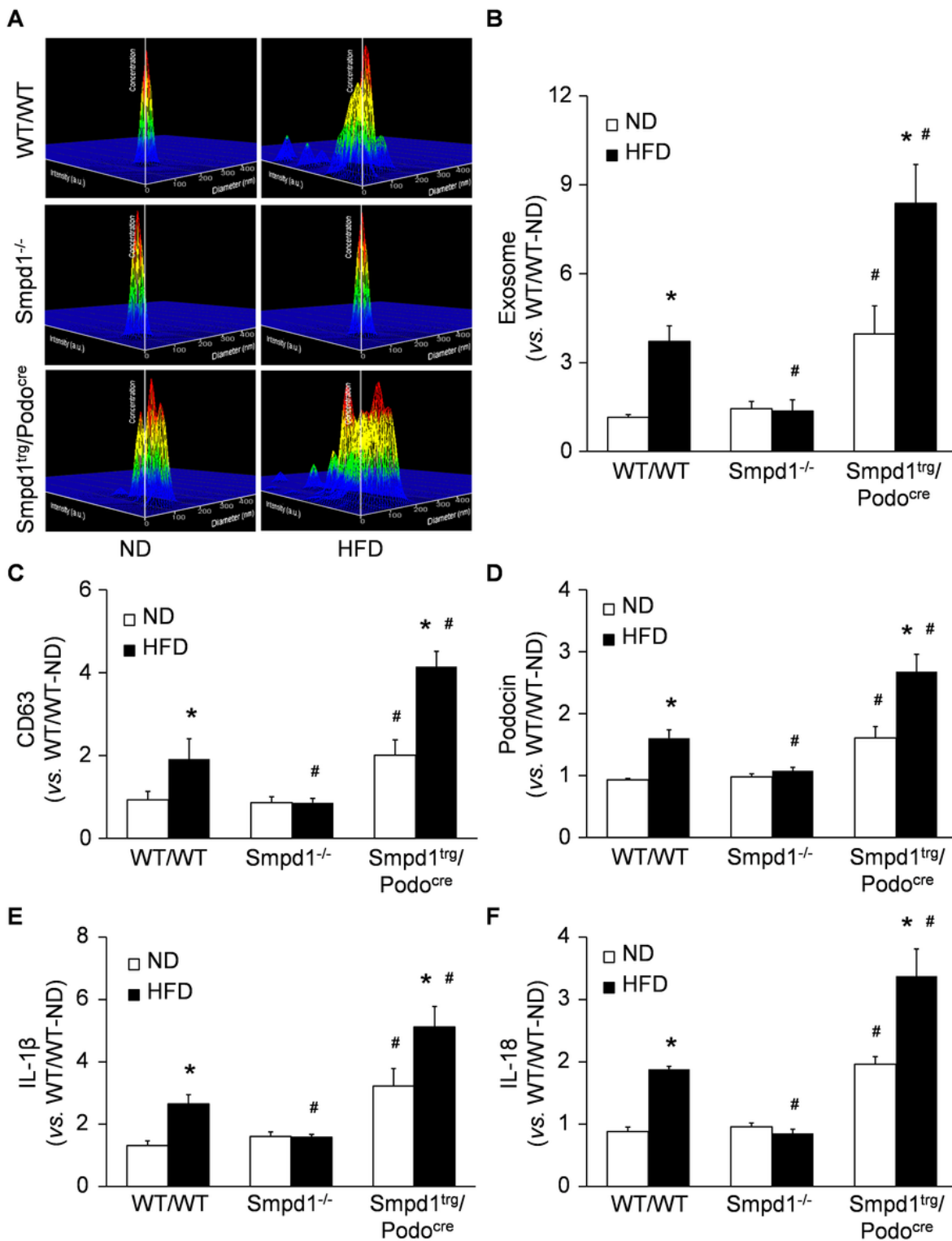


Figure 2

Elevation of inflammatory exosome release during obesity. A. Representative images and summarized data showing the urinary exosome excretion in different groups of mice. The x axis is diameter (nm), the y axis is concentration, the z axis is intensity (a.u.). B. Summarized data showing the urinary exosome excretion in different groups of mice (n=8). C. CD63 in urinary exosomes in different groups of mice (n=6-8). D. Podocin in urinary exosomes in different groups of mice (n=8). E. IL-1 β in urinary exosomes in different groups of mice (n=6-8). F. IL-18 in urinary exosomes in different groups of mice (n=8). * P<0.05 vs. ND group. # P<0.05 vs. WT/WT group.

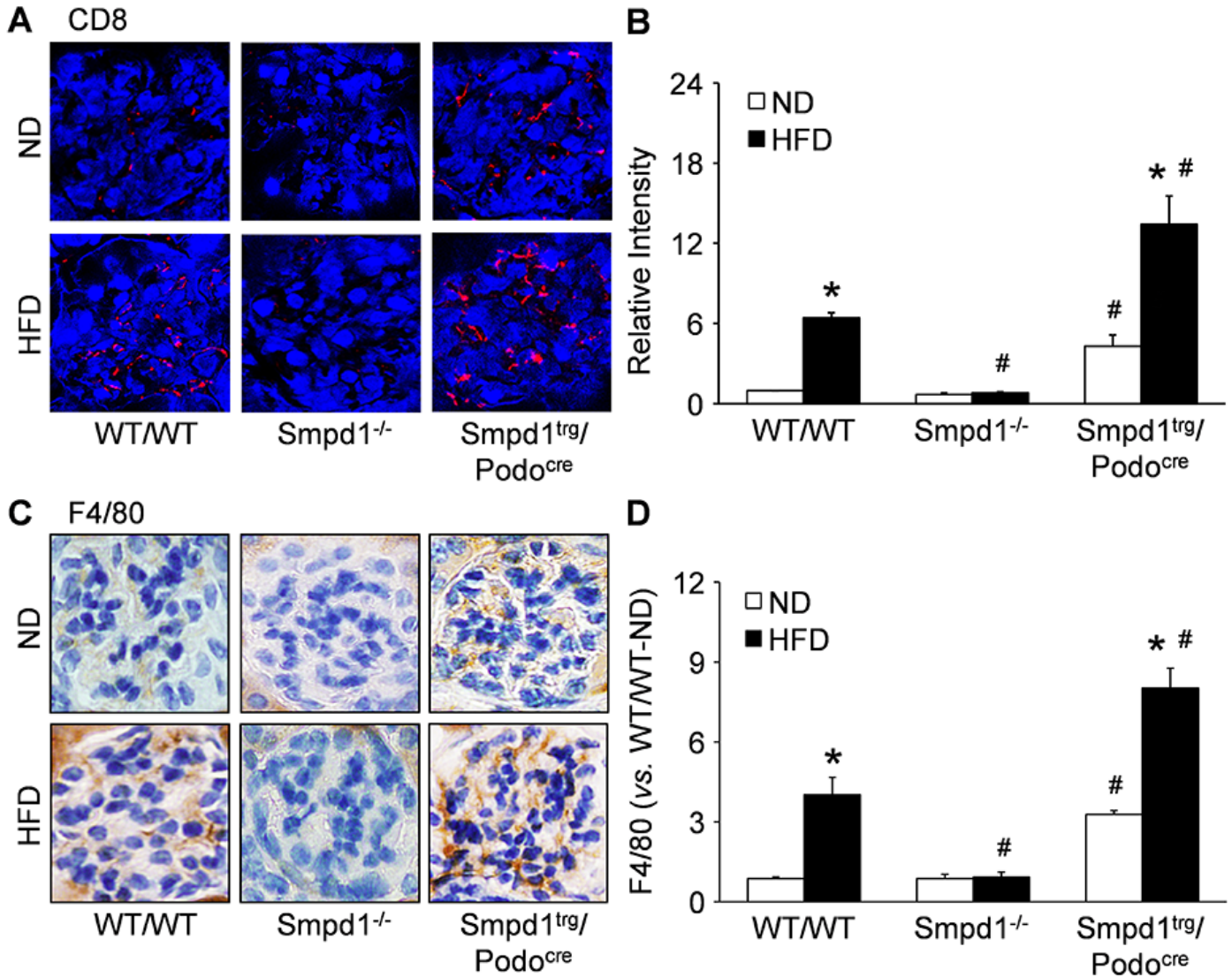


Figure 3

Obesity-induced immune cell infiltration in glomeruli determined by ASM activity in podocytes. A. Representative images and summarized data showing the immunofluorescent staining of CD8 in glomeruli of different groups of mice (n=3). B. Representative images and summarized data showing the

immunohistochemical staining of F4/80 in glomeruli of different groups of mice (n=6). * P<0.05 vs. ND group. # P<0.05 vs. WT/WT group.

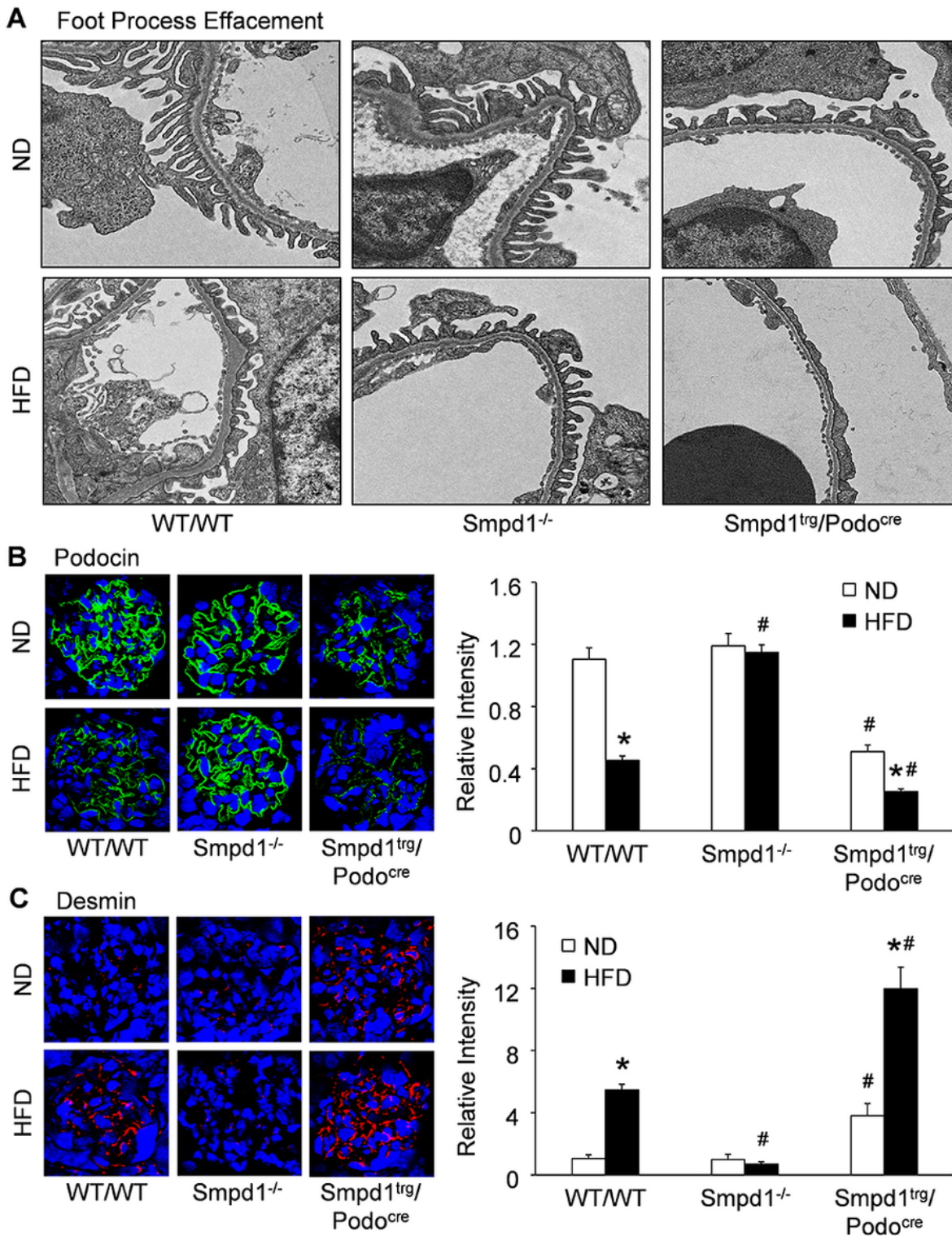


Figure 4

Contribution of ASM activity to podocyte injury during obesity. A. Representative electron microscopic images showing foot processes in podocytes of different groups of mice. B. Representative images and

summarized data showing the immunofluorescent staining of podocin in glomeruli of different groups of mice (n=3-5). C. Representative images and summarized data showing the immunofluorescent staining of desmin in glomeruli of different groups of mice (n=3-5). * P<0.05 vs. ND group. # P<0.05 vs. WT/WT group.

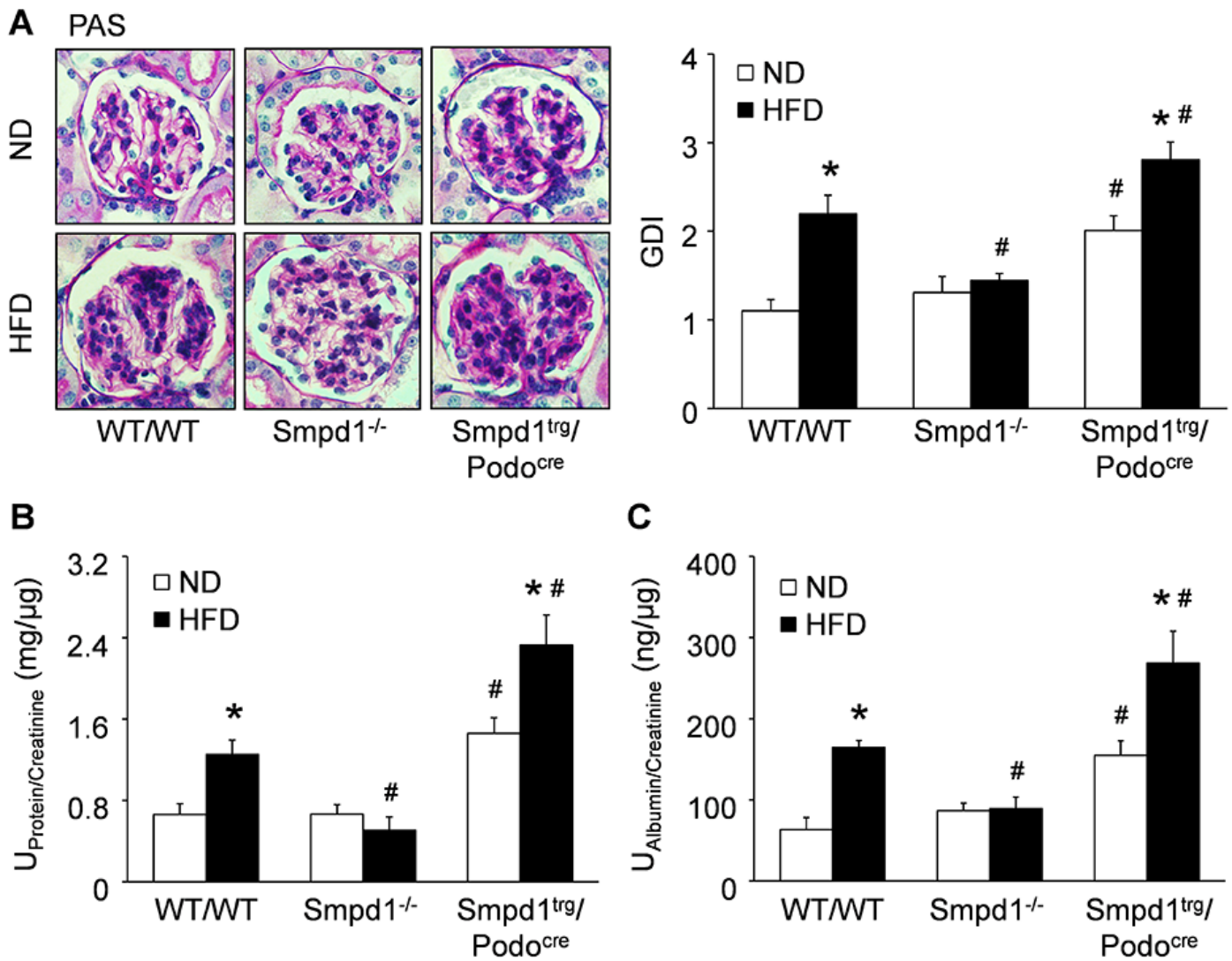


Figure 5

Glomerular damage and proteinuria prevented by Smpd1 gene deletion. A. Representative images and summarized data showing the glomerular morphological changes (periodic acid-Schiff staining) of different groups of mice (n=4-6). B. Urinary protein excretion of different groups of mice (n=7-8). C. Urinary albumin excretion of different groups of mice (n=6-8). * P<0.05 vs. ND group. # P<0.05 vs. WT/WT group.

A NLRP3 vs. ASC

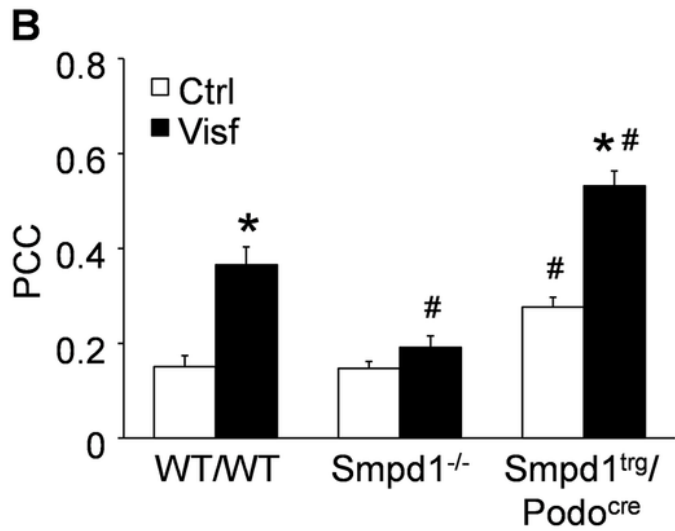
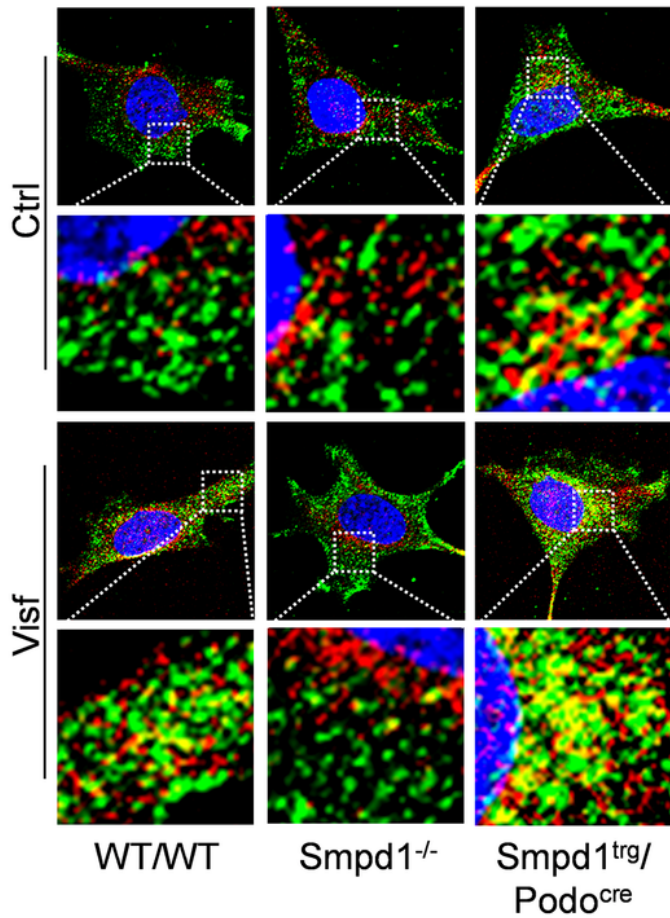


Figure 6

Visfatin-induced NLRP3 inflammasome activation in podocytes. A. Representative images showing the colocalization of NLRP3 and ASC in different groups of podocytes. B. Summarized data showing the colocalization of NLRP3 and ASC in different groups of podocytes (n=6). * P<0.05 vs. Ctrl group. # P<0.05 vs. WT/WT group.

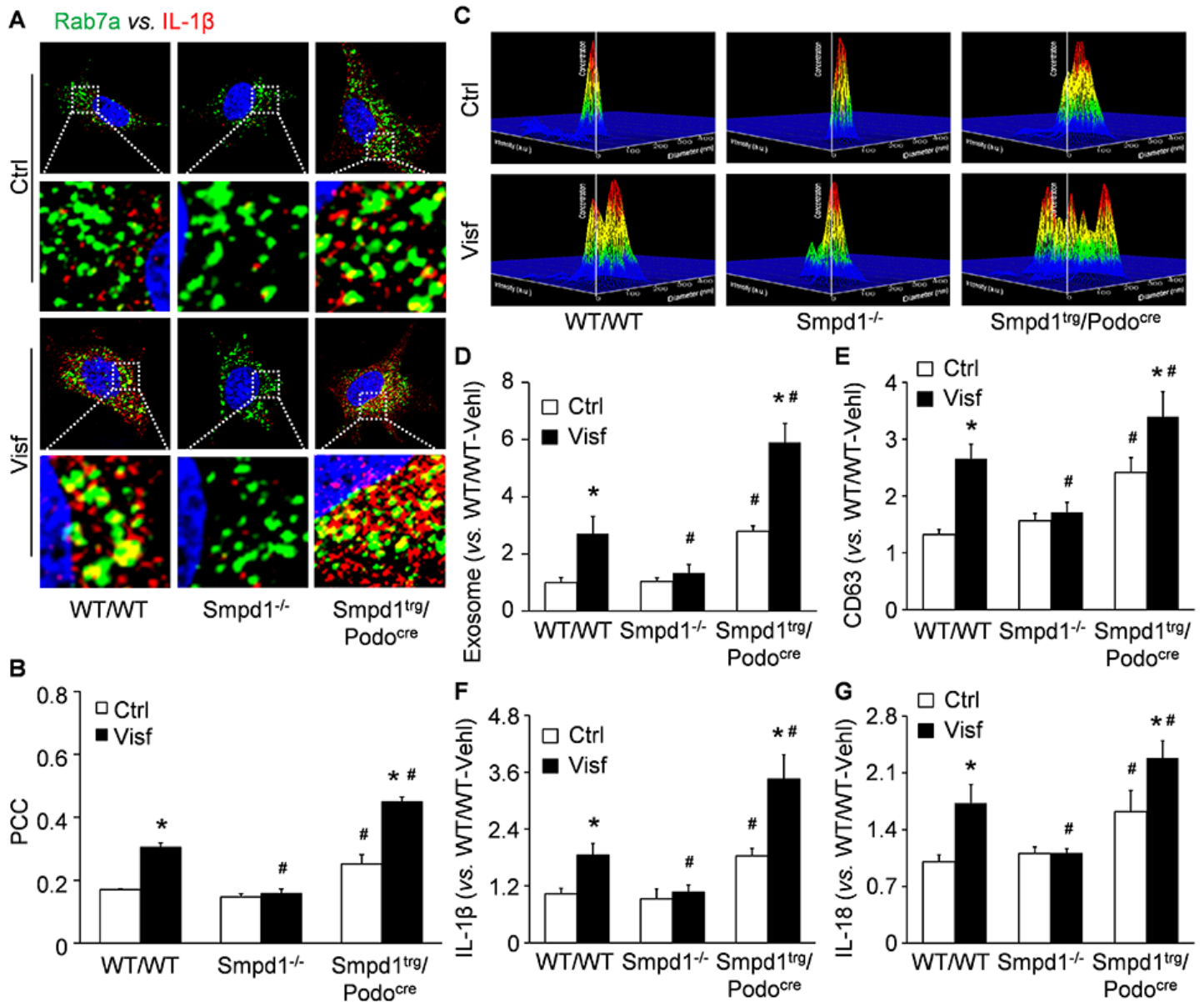


Figure 7

Enhancement of inflammatory exosome release from podocytes by visfatin. A. Representative images showing the colocalization of Rab7a and IL-1 β in different groups of podocytes. B. Summarized data showing the colocalization of Rab7a and IL-1 β in different groups of podocytes (n=5-6). C. Representative images and summarized data showing the exosome release from different groups of podocytes. The x axis is diameter (nm), the y axis is concentration, the z axis is intensity (a.u.). D. Summarized data showing the exosome release from different groups of podocytes (n=6). E. CD63 in exosomes released from different groups of podocytes (n=7-8). F. IL-1 β in urinary exosomes in different groups of mice (n=7). G. IL-18 in exosomes released from different groups of podocytes (n=7-8). * P<0.05 vs. Ctrl group. # P<0.05 vs. WT/WT group.

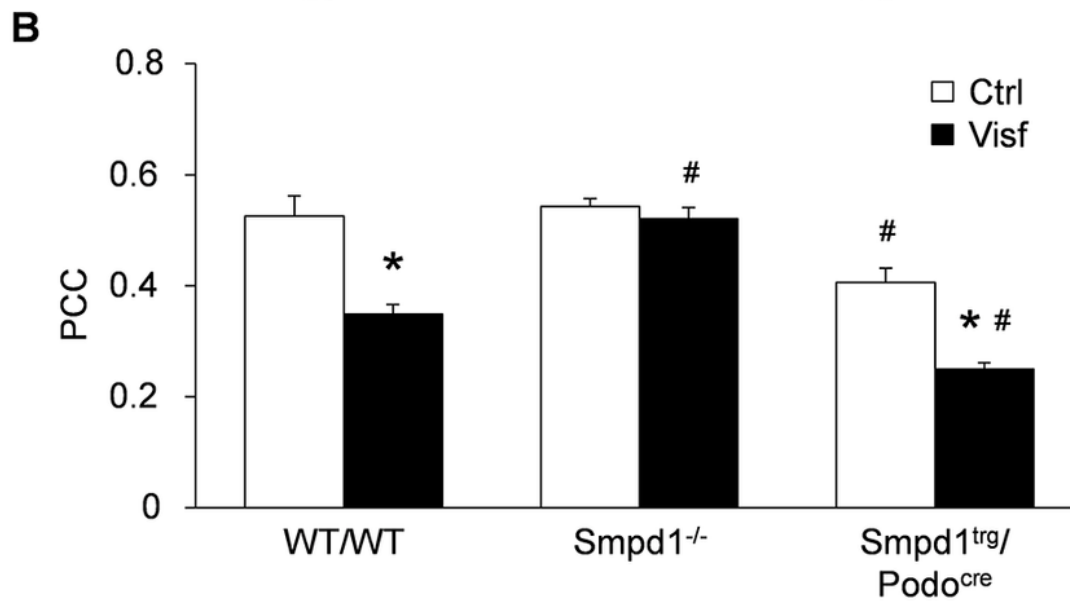
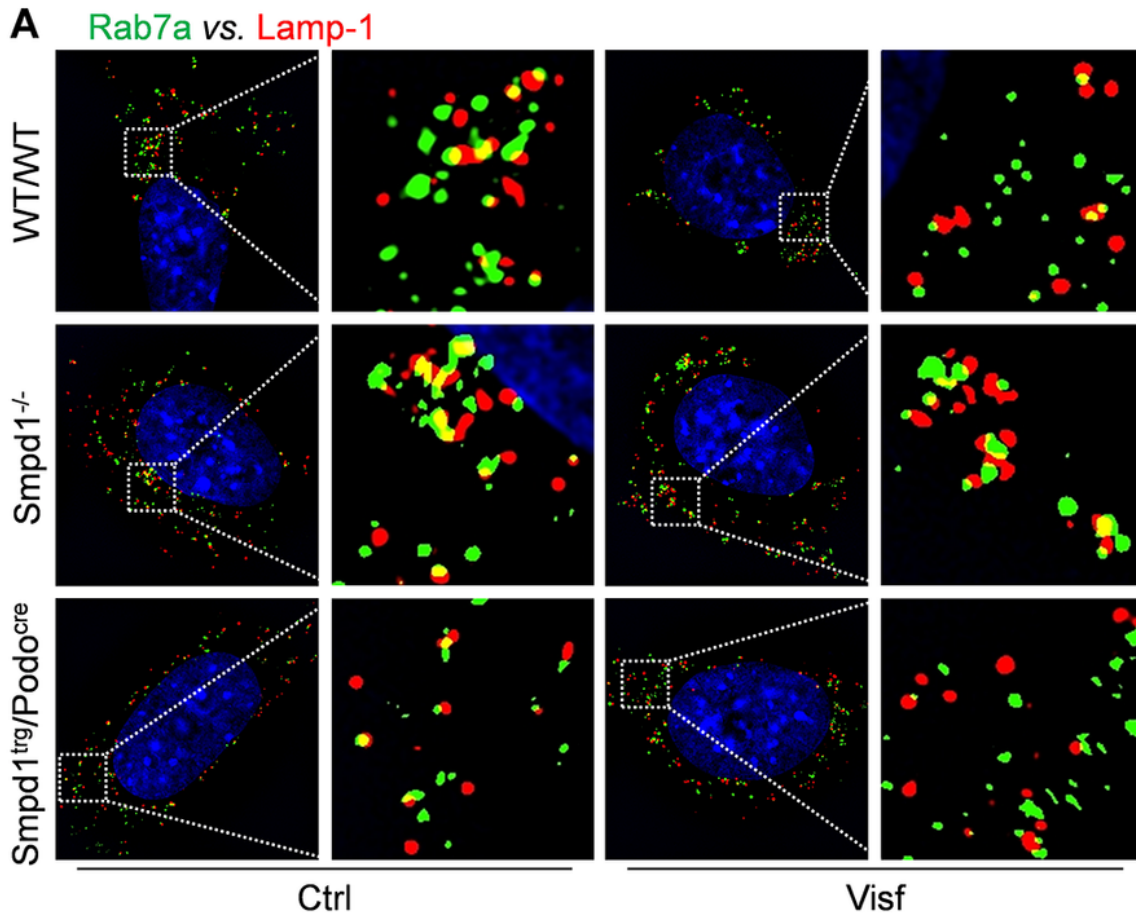


Figure 8

Inhibition of lysosome-MVB interaction in podocytes by visfatin. A. Representative images showing the colocalization of Rab7a and Lamp-1 in different groups of podocytes. B. Summarized data showing the colocalization of Rab7a and Lamp-1 in different groups of podocytes (n=6-8). * P<0.05 vs. Ctrl group. # P<0.05 vs. WT/WT group.